Journal of Solar Energy Research (JSER)

Journal homepage: www.jser.ut.ac.ir

Comprehensive Investigation of Parabolic Trough Collectors for Heating Water in the Algerian Sahara: Experimental and Theoretical Perspectives

Sarah Regragui[a, *], Rachid Maouedj[b], Ali Benatiallah[a], Yacine Marif[c]

[a]*Energy, Environment and Information Systems Laboratory Ahmed Draïa University, Adrar, Algeria*
[b]*Renewable Energy Research Unit in the Saharan Environment URERMS, Adrar, Algeria*
[c]*New and Renewable Energy Development Université Kasdi Merbah, Ouargla, Algeri*

ARTICLE INFO

Article Type:

Research Article

Received:2026.01.07
Accepted in revised form:2026.06.02

Keywords:
Parabolic trough collector; Water heating; Saharan climate; Thermal efficiency; Experimental validation; Finite difference

A B S T R A C T

This study presents both experimental and simulation-based analyses of an affordable, compact parabolic trough collector designed for water heating in the arid Saharan climate of Adrar, southern Algeria. Experiments were conducted in June under peak solar irradiation of approximately 800 W/m². A transient one-dimensional model grounded in energy balance equations and an implicit finite difference scheme was developed and validated against experimental data, showing a maximum deviation below 5%. The collector achieved a peak thermal efficiency of about 80% at solar noon, while daily experimental efficiency ranged from 55% to 75%. At a debit rate of 0.1 kg/s, the temperature of expulsed water approached approximately 75°C however, it declined at elevated flow rates owing to the decrease staying duration of the liquid incorporated in the system. These results confirm that lower mass flow rates enhance thermal performance. Furthermore, this work provides a rare experimentally validated transient model for compact PTC systems operating under extreme Saharan conditions, where high ambient temperatures significantly influence heat-loss mechanisms, thereby supporting improved concept and enhancement of small-scale solar thermal setups in arid regions.

1. Introduction

Over recent decades, international energy usage has elevated drastically due to demographical growth and industrial development. Fossil carburant counting oil, coal, and natural gas persist as the predominant cause to the international energy portfolio, constituting approximately 80% of aggregate energy consumption [1]. The extensive dependence on fossil fuels has precipitated a marked escalation in

*Corresponding Author Email: reg.sarah@univ-adrar.edu.dz

Cite this article: Sarah, R., Rachid, M., Ali, B. and yacine, M. (2026). Comprehensive Investigation of Parabolic Trough Collectors for Heating Water in the Algerian Sahara: Experimental and Theoretical Perspectives. Journal of Solar Energy Research, 11(2), 3010-3026. doi: 10.22059/jser.2026.409103.1704

DOI: 10.22059/jser.2026.409103.1704

greenhouse gas emissions, thereby exacerbating climate change and its attendant environmental consequences. Consequently, the tilt from conventional fossil carburant toward renewable energy reserves has emerged as a global imperative.

Photovoltaic power is broadly reknowned as among the highly demanded and viable reusable energy sources, given its vast availability and enduring sustainability. Its immense potential has the capacity to far exceed global energy consumption, positioning it as a crucial element in curtailing fossil fuel dependency and fulfilling sustainable energy objectives[2]. Solar energy represents an environmentally benign technology and one of the foremost renewable and sustainable energy sources, substantially contributing to the realization of sustainable development objectives within the energy sector. The vast quantities of solar radiation available daily render it an exceptionally viable resource that can be harnessed across diverse geographical regions worldwide[3]. The quantity of solar energy incident upon the terrestrial surface substantially surpasses contemporary global energy consumption by multiple orders of magnitude, thereby establishing solar radiation as one of the foremost viable reusable power reservoir. Countries in the southern Mediterranean basin, in particular, receive exceptionally elevated amounts of direct solar irradiation, positioning solar power as a strategically viable solution for meeting both local and regional energy requirements. The Mediterranean regions demonstrate considerable solar potential, as indicated by their mean yearly solar irradiation values, which commonly surpass 2,000 kWh/m² and rank them among the planet's foremost solar-abundant zones[4]. Within this framework, focused solar potency technologies have been delimited as particularly well-suited to Algeria's abundant solar resources, offering a viable pathway toward reducing dependence on conventional energy sources[5] Accordingly, transitioning toward solar-based energy systems is widely regarded as a cornerstone of sustainable development strategies aimed at curbing greenhouse gas emissions and diversifying the regional energy mix [6] .

Algeria has highly favorable climatic conditions for solar energy utilization, characterized by high solar irradiation levels, low humidity, and limited annual rainfall, along with vast open land areas suitable for large-scale installations [6] The southern Saharan region of Algeria is particularly endowed with exceptional solar resources, making it one of the highly attractive locations for solar thermal utilisation in North Africa. The sunshine duration across the entire Algerian territory exceeds 3,000 hours per year and can reach up to 3,500 hours per year in the Sahara, with daily irradiation surpassing 10 hours in the southern regions. The mean yearly photovoltaic radiation exposure across Algeria varies roughly between 1,700 kWh/m² in locations of the north to above 2,200 kWh/m² in desert southern zones , underscoring the nation's considerable capacity for large-scale solar energy initiatives[7].

Solar water heating constitutes one of the earliest and most widely implemented utilisations of solar thermal energy. Early systems relied on simple black-painted storage tanks to absorb and retain solar heat. Over time, technological advancements have significantly improved collector designs, materials, and thermal performance [8]. Continuous innovations aimed at enhancing solar absorption and minimizing thermal losses have contributed to substantial improvements in overall system efficiency [9] .

In solar thermal systems, the solar collector serves as the primary component by absorbing iminent solar rays and transducing it into thermal potency to heat an active fluid such as oil, water, or air[10]. Various solar collector technologies have been developed, including flat-plate, evacuated tube, concentrating, and unglazed low-temperature collectors. The selection of an appropriate collector type is contingent upon the specified operating temperature range and the intended application.

Among concentrating solar thermal advances, parabolic trough receptors are recognized as among the most established and widely deployed systems. The operational mechanism of these systems is based on parabolic reflectors that focus direct solar radiation onto a container tube, thereby increasing the calorific energy absorbed by the heat liquid. Owing to their concentrating nature, PTCs are generally capable of functioning at temperatures englobed between 120 to 250°C, rendering them appropriate for industrial process heating applications, steam generation, and domestic hot water production. Their relatively simple design, combined with high optical efficiency and reliable operation, has contributed to their extensive deployment in medium-temperature solar applications [11].

Solar thermal water heating systems have gained widespread adoption across a broad spectrum of applications. Applications encompass space heating and cooling in residential and commercial structures, seawater desalination, drying and preservation of foodstuffs, and the incorporation of photovoltaic thermal energy into multiple industry chain process heating operations. The adaptability and economic viability of these technologies have

positioned them as a fundamental component in advancing sustainable energy transitions [12].

The calorific action of parabolic trough collectors (PTCs) is influenced by several key factors, including optical losses related to reflectivity and transmissivity limitations, thermal losses through convection and radiation, as well as geometric imperfections such as receiver misalignment and tracking errors, which can significantly reduce the overall collector efficiency [13]. A major design challenge is achieving an optimal balance between aperture size and system efficiency, since larger apertures may increase thermal losses, while smaller apertures may reduce optical concentration and solar interception. Therefore, maximizing long-term PTC performance requires careful design optimization and appropriate operating conditions.

Recent studies have reported notable improvements in PTC thermal performance through receiver design modifications and enhanced heat transfer techniques. The integration of concentric tube designs with hybrid nanofluids and optimized fin structures has demonstrated significant increases in thermal efficiency, highlighting the effectiveness of combined passive enhancement strategies [14].

To reduce thermal losses, PTC absorber tubes are commonly enclosed within a glass envelope, which minimizes convective heat loss and improves overall thermal performance. Previous studies have reported that the use of a glass envelope can significantly enhance outlet water temperature and temperature gradients [15] Furthermore, comparative analyses between mirror and aluminium foil reflectors have demonstrated that mirror reflectors provide superior optical performance, resulting in higher peak temperatures and improved thermal efficiency [16].

Several experimental investigations have explored the application of advanced working fluids and receiver designs to improve parabolic trough collector performance. For example, an experimental assessment involving a U-tube absorber with nickel ferrite nanofluid indicated that higher mass flow rates can substantially enhance the configuration overall thermal efficiency [17] In addition, the incorporation of nanoparticles into the heat exchange liquid was reported to enhance the convective heat transfer coefficient; however, it may also lead to higher pressure drops within the receiver tube [18] .

Further investigations have examined innovative PTC configurations incorporating U-tube receivers and nanofluids. These studies indicated that nanoparticle size and flow rate are key parameters affecting the calorific proficiency of the configuration [19]. Moreover, lumped parameter modelling approaches have been successfully applied to simulate PTC thermal behaviour, and numerical results obtained using MATLAB showed good agreement with experimental observations, demonstrating the usefulness of such models for design and performance prediction [20].

Advanced numerical investigations have also been conducted using three-dimensional thermo-hydrodynamic models to analyze PTC performance. For example, a two-fluid approach was applied to simulate direct steam generation in a PTC-integrated steam plant, enabling the evaluation of key thermal–hydraulic parameters under different solar irradiation conditions, including peak solar noon and surrounding time intervals [21].

Various numerical tools and software applications have been utilized to simulate the thermal performance of parabolic trough collectors [10]. For example, advanced thermal modelling studies based on the Engineer Equation Solver (EES) have incorporated the principal heat exchange mechanisms—conduction, convection, and radiation—to achieve enhanced simulation accuracy.

Exergy analysis has also been employed to assess the consequence of actionable and ecological settings on the aptitude of parabolic trough collectors (PTCs). These studies revealed that the absorber tube is typically the main source of exergy destruction due to irreversible heat transfer processes occurring within the receiver [22] [23] . Based on these findings, several enhancement tactics were proposed to enhance the thermodynamic aptitude of next-generation PTC systems.

Several studies have investigated parabolic trough collector (PTC) systems operating in medium-temperature ranges, with particular emphasis on different operating strategies and control approaches. The results indicated that solar thermal systems can supply a significant portion of thermal energy demand in various applications, especially when properly optimized under realistic operating conditions [24] [25] .

Experimental investigations have also focused on evaluating the optical capacities of parabolic trough collectors (PTCs) and analyzing the influence of engineering design parameters on thermal efficiency. The results demonstrated that absorber material properties and geometric characteristics play a critical role in determining heat capture effectiveness [26] Furthermore, thermal simulations of PTC configurations have been conducted to improve system performance and design accuracy [27] The findings of these studies underscore the necessity of

optimizing both optical and thermal parameters to augment collector efficiency.

The application of porous media in concentration solar power (CSP) systems were studied as an effective way to boost heat transfer and enhance thermal efficiency[28] .Numerical meth ods, such as 2D and 3D CFD simulations, are commonly used to examine heat losses, flow dynamics, and thermal dissipation in the receiver tube and glass envelope. [29] Furthermore, transient numerical methods such as the Crank–Nicolson scheme have been employed to resolve the controlling formula for heat transduction in solar thermal systems. [30], Advanced computational fluid dynamics software packages, such as FLUENT and STAR-CCM+, have also been widely employed to simulate intricate processes including active steam formation in parabolic trough receivers, with outcomes demonstrating close alignment to experimental observations[31] [32] .

Parabolic trough collector systems are extensively acknowledged for their superior thermal efficiency and their appropriateness for solar applications operating at moderate temperatures. Owing to their capacity to concentrate direct solar radiation, these systems constitute a viable approach for hot water production in regions characterized by elevated solar potential. However, the thermal potency of compact parabolic trough collector environment functioning under severe climatic environments, such as those found in the Saharan region, remains insufficiently documented in the literature. In addition, simplified numerical models capable of accurately predicting transient system behavior are essential for performance assessment and design optimization.

Agagna et al. [13] demonstrated that geometric and optical errors in PTC systems, including receiver misalignment and tracking inaccuracies, can lead to significant reductions in both optical and overall thermal efficiency, underscoring the importance of precise manufacturing and installation tolerances in achieving reliable collector performance. Moreover, recent solar water heating developments have introduced advanced receiver configurations and control-oriented designs; however, further investigations under harsh outdoor conditions and for compact low-cost systems remain required to support decentralized hot water applications [33]. In addition, up-to-date review papers underline that, despite extensive progress in receiver enhancement and numerical modeling, practical gaps persist regarding validated simplified transient models and performance assessment of small-scale PTC units operating under extreme climates, Furthermore, Kim et al. [34] reviewed recent design innovations and optimization efforts in parabolic trough collectors and highlighted continued evolution in receiver enhancement, thermal modelling, and system-level optimization. Numerous investigations have examined the operational efficiency of parabolic trough collector-founded photovoltaic thermic energy plantation across various Algerian regions. A computational modeling of a 100 MW PTC solar thermic power plantation was conducted across three representative Algerian sites — Adrar, Ghardaïa, and Hassi Messaoud — evaluating annual direct normal irradiance (DNI) as a key performance parameter. The results demonstrated the strong potential of these regions for large-scale solar thermal electricity generation [35] .

Accordingly, the current study seeks to experimentally and numerically evaluates the thermal activity of a compact parabolic trough collector operating in the climatic configuration of Adrar in southern Algeria.

An implicit finite difference discretization is utilized to develop a one-dimensional transient thermal model that simulates heat transfer phenomena within the tube receiver, glass frame, and working fluid. The numerical model is validated against experimental measurements obtained under high solar irradiation conditions. Furthermore, the consequence of mass flow rate and collector dimensions on outlet water temperature and thermal efficiency are systematically examined. The findings of this work provide practical guidelines for optimizing small-scale PTC systems intended for residential and moderate industrial hot water applications in arid regions

2. Materials and Methods

2.1. System Description

The PTC system employed in this investigation comprises a parabolic reflective mirror, an evacuated cylindric absorber, a metallic supporting farmwork, and a uniaxial solar tracking mechanism. Figure 1 presents a schematic diagram of the experimental apparatus.

The construction process started with the fabrication of the metallic frame, which provided the mechanical support for the collector. Subsequently, the parabolic reflector and receiver were installed in order to maximize solar radiation concentration along

the focal line. Finally, the absorber tube was mounted to complete the assembly of the PTC system.

The parabolic reflector measures 1.4 m in length and 0.9 m in height, with the mirror structure exhibiting a thickness of 4 mm. This configuration facilitates the concentration of incident solar radiation along the focal line, where the receiver tube is situated. The absorbed concentrated solar energy raises the absorber temperature, enabling subsequent heat transduction to the heat transfer fluid and thereby elevating the outlet fluid temperature. The principal geometrical index of the PTC configuration is summarized in Table 1.

Table 1. Thermal, geometric, and optical characteristics associated with the PTC

Parameters	Unit	Estimated values
evacuated tube properties		
Absorber length	m	1.4
Inner absorber diameter (D_1)	cm	0.035
Outer absorber diameter (D_2)	cm	0.04
Absorptivity of absorber (α_{ab})	-	0.95
Absorptivity of glass (α_g)	-	0.02
The absorber density (ρ_{ab})	kg/m³	8920
The density of glass (ρ_g)	kg/m³	2530
glass Emittance envelope (ε_g)	-	0.88
absorber Emittance (ε_{ab})	-	0.05
Glass Envelope transmissivity (τ_g)	-	0.95
The absorber's specific heat	J/ (kg. K)	385
Reflector properties		
Reflector reflectance	-	0.935
Intercept factor	-	0.90
Glass's specific heat capacity (Cp_g)	J/(kg·K)	830
Mirror reflectivity (ρ_r)	-	0.95
Collector material	2 mm Galva Metal	

2.2. Installation process

The parabolic trough collector system was experimentally designed, constructed, and installed at the Renewable Energy Research Unit in the Saharan Environment, CDER, Adrar, Algeria. To optimize solar energy capture, the collector was equipped with a single-axis pursuing system aligned along the north–south direction This arrangement allows the enables continuous monitoring of the sun's apparent east-to-west path, thereby maximizing solar radiation incidence on the reflector surface. Outdoor experimental evaluations were performed during June under representative Saharan climatic conditions. The parameters that follows were monitored continuously:

- Intensity of Direct photovoltaic Radiation
- Temperature of Ambient air
- interring and outlet temperatures of the water
- Mass flow rate of the water

The thermal performance efficiency of the PTC reached calculated on the basis the measured data, particularly for the representative day of June 21, which corresponds to peak solar irradiation conditions

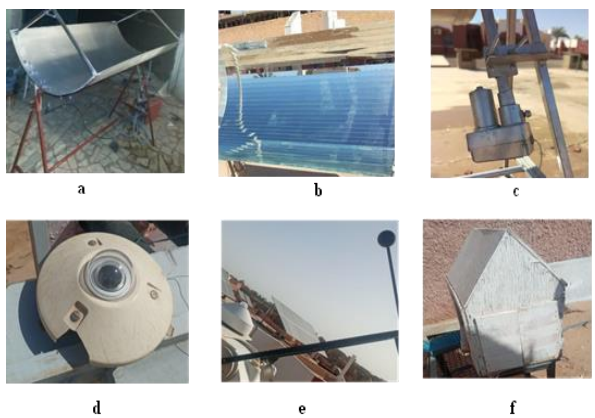

Figure 1. (a) producing the designed PTC, (b) pasting mirrors, (c) tracking system (d) Pyranometer used to measure global radiation (e) measuring diffuse radiation with the ball(f) thermocouple for ambient temperature measurement

2.3. Experimental Measurements and Data Acquisition

Outdoor experiments were conducted under real climatic conditions in Adrar, Algeria, using a North–

South oriented PTC equipped with a uniaxial tracking setup to guaranty maximum solar interception. The direct normal irradiation (DNI) was measured via a calibrated pyranometer installed in the same plane as the collector aperture. Ambient temperature (T_{amb}) was recorded using a shaded K-type thermocouple to avoid direct solar exposure. The inlet temperature (T_{in}) and outlet temperature (T_{out}) of the working fluid were recorded using calibrated K-type thermocouples equipped at the absorber tube entrance and exit, ensuring accurate measurement of the fluid temperature increase across the collector. In addition, the mass flow rate (ṁ) was determined through a calibrated debit meter.

The measurement accuracy was ±1°C for temperature sensors, ±5 W/m² for solar irradiation, and ±2% for the mass flow rate. All parameters were recorded at regular time intervals to capture the transient thermal behaviour of the system under varying solar conditions. These measurements were subsequently used to assess the mediate thermal proficiency and to validate the numerical model.

2.4. Thermal Effectiveness coefficient Calculation

The instantaneous thermal efficiency of the parabolic trough collector was performed by calculating the proportion of useful thermal power quired by the heat transfer liquid to the incident solar power on the collector aperture surface.
The useful heat gain is as follows [36]:

$$Q_u = \dot{m}\, Cp\left(T_{out} - T_{in}\right) \quad (1)$$

we have ṁ denotes the mass flow rate (kg/s), Cp represents the specific heat ability of water (J/kg·K), and T_{out} and T_{in} correspond to the outlet and inlet temperatures (°C), respectively.
The incoming solar power on the collector aperture surface is given by [37]

$$Q_s = \text{DNI}\ A_a \quad (2)$$

where DNI is the measured direct normal irradiation (W/m²) and Aa is the collector aperture surface (m²).
Therefore, the thermal efficiency is evaluated as [38]:

$$\eta_{th} = \frac{Q_u}{Q_s} \quad (3)$$

This formulation provides a direct and reliable indicator of collector performance under varying solar radiation and environmental conditions.

3. Numerical Model Development

3.1.PTC heat transfer analysis and numerical modelling

The calorific behavior of the PTC was examined across different mass flow rates and actual solar immittance conditions. A dynamic unidimensional heat transduction model was formulated for the Heat Collection Element, drawing upon the preservation of mass and power. The energy balance incorporates incident direct solar radiation, optical losses between the reflector and receiver, thermal reductions from the absorber and glass cover, and the effective thermal energy absorbed by the heat transfer fluid.

The receiver was segmented into multiple control volumes along its axial length to establish the governing equations. Conservation equations were then applied to analyze each segment separately. Fig. 2 and Fig. 3 provide schematic illustrations of the receiver cross-section and a representative control volume.

To support the mathematical formulation of the heat transfer model, the below hypothesis was adopted:

- Axial heat conduction within the receiver cylinder and glass cover is disregarded.
- We hypothesized that solar immittance reflected by the concentrator is specular and evenly distributed along the absorber length.
- Heat losses from the receiver ends are negligible.
- Thermophysical properties of all materials are supposed constant.
- The heat transfer fluid is supposed to be incompressible and to undergo steady one-dimensional flow.
- Temperature repartition on the direction of the circumferential path of the receiver is homogeneous.
- The annular region separating the absorber tube from the glass envelope is filled with air maintained at a predetermined pressure.

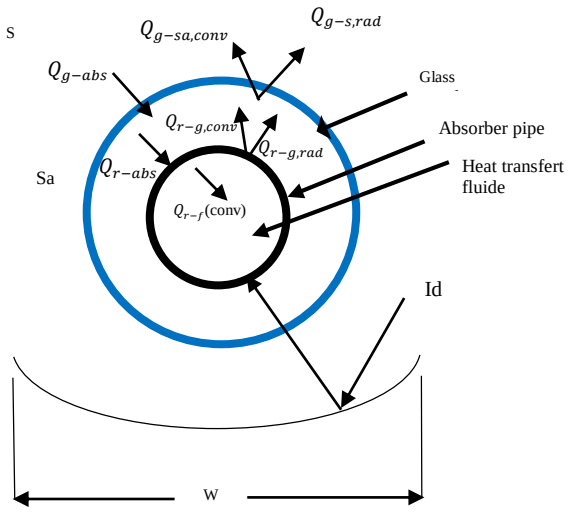

Figure 2. An illustration of the control volume and photovoltaic receiver in cross-section

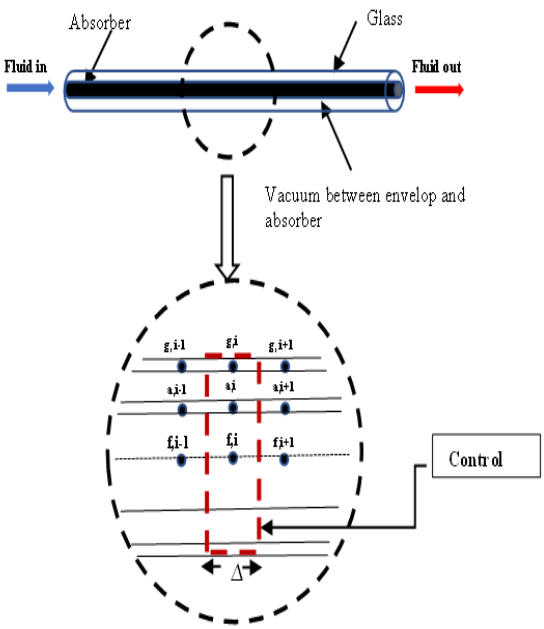

Figure 3. An illustration of the control volume and solar receiver in cross-section

3.2. Heat exchange – Case of Absorber surface / Heat Transfer liquid

The heat transfer between the absorber tube and the heat transfer fluid (HTF) is predominantly regulated by convection occurring along the absorber's inner wall. This process is described by applying the energy conservation principle to a differential fluid control volume, the following expression can be obtained [39]:

$$\left(A_f \rho_f Cp_f\right)\frac{dT_f}{dt} = -\left(\frac{\dot{m}_f Cp_f}{\Delta x}\right)\frac{dT_f}{dt} + A_f k_f \frac{d^2T_f}{dx^2} + Q_{r-f,conv} \quad (4)$$

Where A_f denotes the fluid cross-sectional surface, ρ_f is the fluid density, and c_{P_f} denotes the exact heat potency of the liquid. $\dot{m}_f$ mass flowing debit of the fluid, and k_f is the thermal conductivity.

The convective heat entered by the heat transferring liquid is expressed as[40].

$$Q_{r-f,conv} = \pi D_{ab(\text{int})} h_u \left(T_{ab} - T_f\right) \quad (5)$$

Where $\boldsymbol{D_{ab(\text{int})}}$ diameter interior of absorber, $\boldsymbol{h_u}$ useful heat transfer coefficients

Useful heat coefficient [41]

$$h_{u(f)} = \frac{k_f}{D_{ab(\text{int})}} Nu_f \quad (6)$$

For laminar flow (Re < 2300), the Nusselt numbers, $N_{U_{f_1}}$ and $N_{U_{f_2}}$ under the boundary conditions of constant wall temperature (which is advised) and constant heat flux, respectively, are as follows [41]

$$Nu_{f1} = \left\{(3.66)^3 + (0.7)^3 + \left(1.6153\sqrt{Re_f Pr_f d} - 0.7\right)^3 + \left(\left(\frac{2}{1+22Pr_f}\right)^{\frac{1}{6}}\sqrt{Re_f Pr_f d}\right)^3\right\} \quad (7)$$

$$Nu_{f2} = \&\left\{(4.354)^3+(0.6)^3+\left(1.953\sqrt[3]{Re_f Pr_f d}-0.6\right)^3 +\left(0.924\sqrt[3]{Pr_f}\sqrt{Re_f Pr_f d}\right)^3\right\}^{\frac{1}{3}} \quad (8)$$

In the transition region ($\mathbf{2300 \leqslant Re \leqslant 4000}$) This equation was proposed by Gnielinski [41]

$$\mathrm{Nu}_f = (1-\gamma)\,\mathrm{Nu}_{(\mathrm{Lam.2300})} + \gamma\,\mathrm{Nu}_{(\mathrm{Turb,4000})} \quad (9)$$

Were:

$$\gamma = \frac{\left(Re_f - 2300\right)}{4000-2300} \quad (10)$$

3.3. Heat transfer: case of glass envelope / environing environment.

In the selected control volume, the energy balance for the glass envelope is formulated as follows [39]:

$$\left(A_g \rho_g Cp_g\right)\frac{dT_g}{dt} = A_g k_g \frac{d^2T_g}{dx^2} + Q_{g\text{-}abs} + Q_{r\text{-}g,conv} + Q_{r\text{-}g,rad} - Q_{g\text{-}s,rad} - Q_{g\text{-}sa,conv} \quad (11)$$

$$Q_{g\text{-}abs} = WI_d \rho_0 \alpha_g \gamma K \quad (12)$$

Where W is the collector width, and ρ_0 reflected surface reflectivity and α_g is the absorbance factor of the glace, and γ is the shape coefficient.

The representation of the incident angle modifier K is [23].

$$K = 1-0.00384(\theta)-0.000143(\theta)^2 \quad (13)$$

The provided equation was used to determine the direct sun radiation Id [42].

$$I_d = I_0 \varepsilon \cos\theta \exp\left(-T_L m_A \delta_R\right) \quad (14)$$

The atmospheric mass m_A, and the integral Rayleigh optical thickness δ_R are determined by [42]

$$m_A = \left[\sin(h)+9.410^{-4}(\sin(h)+0.0678)^{-1.253}\right]^{-1} \quad (15)$$

$$\frac{1}{\delta_R} = 6.6296+1.7513m_A-0.1202m_A^2+0.0065m_A^3-0.00013m_A^4 \quad (16)$$

$$Q_{r\text{-}g,conv} + Q_{r\text{-}g,rad} = \pi D_{ab(ext)} h_{(\mathrm{int})}\left(T_r - T_g\right) \quad (17)$$

$$Q_{g\text{-}s,rad} + Q_{g\text{-}sa,conv} = \pi D_{g(ext)}\left[h_{c(ext)}\left(T_g - T_{sky}\right)+h_{r(ext)}\left(T_g - T_a\right)\right] \quad (18)$$

The correlation by García-Valladares and Velázquez [43] ,[23] is advised for estimating natural convection between the exterior air in windless conditions and the glass envelope. The physical characteristics of the surrounding air were determined based on the average temperature (Ta+Tg)/2, and Eq. (١٦) defines the external convection heat transfer coefficient.

$$h_{c(\mathrm{ext})} = \left[0.6+0.387\left(\frac{Ra_{\mathrm{air}}}{\left(1+\left(\frac{0.559}{Pr_{\mathrm{air}}}\right)^{\frac{9}{16}}\right)^{\frac{16}{9}}}\right)^{\frac{1}{6}}\right]^2 \frac{k_{\mathrm{air}}}{D_{g(ext)}} \quad (19)$$

When wind is present, convection transitions to a forced mode, and Zhukauskas's correlation is recommended. Here, the ambient temperature is used to calculate the exterior air's physical characteristics, whereas Pr_g is assessed at the glass envelope

temperature, thereby determining the external convection heat transfer coefficient [44]

$$h_{c(ext)} = C\,\mathrm{Re}_{air}^{n}\,P_{air}^{m}\left(\frac{\mathrm{Pr}_{air}}{\mathrm{Pr}_{g}}\right)^{\frac{1}{4}}\frac{k_{air}}{D_{g(ext)}} \qquad (20)$$

According to [23] [45]

$$1<\mathrm{Re}_{air},\ 40\Rightarrow C=0.75,n=0.4 \qquad (21)$$

$$40<\mathrm{Re}_{air},\ 10^{3}\Rightarrow C=0.51,n=0.5 \qquad (22)$$

$$10^{3}<\mathrm{Re}_{air},\ 2\times10^{5}\Rightarrow C=0.26,n=0.6 \qquad (23)$$

$$2\times10^{5}<\mathrm{Re}_{air},\ 10^{6}\Rightarrow C=0.076,n=0.7 \qquad (24)$$

$$m=\begin{cases}0.37 & \mathrm{Pr}_{air},\ 10\\ 0.36 & \mathrm{Pr}_{air}>10\end{cases} \qquad (25)$$

The pressure within the annular space linking the receiver and the glass cover determines the inner convection heat exchange coefficient $h_c(\mathrm{int})$ When the annular pressure is below 0.013 Pa, $h_c(\mathrm{int})$ is assumed to be zero [43] . However, if the annular pressure exceeds 0.013 Pa, two horizontal, concentric cylinders and their natural convection relations are used to estimate $h_c(\mathrm{int})$ [23])[43]. The physical properties of the air within the annulus are calculated at the average temperature.

$$\mathrm{h_{c\,(int)}}=\frac{2\mathrm{k_{eff}}}{\mathrm{D_{ab\,(ext)}}\ln\left(\frac{\mathrm{D_{g\,(int)}}}{\mathrm{D_{ab\,(ext)}}}\right)} \qquad (26)$$

with

$$k_{eff}=0.386k_{a}\left(\frac{\mathrm{Pr}_{a}}{0.861+\mathrm{Pr}_{a}}\right)^{\frac{1}{4}}\left(Ra_{c}\right)^{\frac{1}{4}} \qquad (27)$$

Were

$$Ra_{c}=\frac{\left(\ln\left(\frac{D_{g(l\,\mathrm{int})}}{D_{ablet}}\right)\right)^{4}}{L_{eff}^{3}\left(D_{ab(ext)}^{-\frac{3}{5}}+D_{g(\mathrm{int})}\right)}\Bigg)^{-\frac{3}{5}}Ra_{eff} \qquad (28)$$

$$L_{eff}=\frac{D_{g(\mathrm{int})}-D_{ab(ext)}}{2} \qquad (29)$$

$$Ra_{eff}=Gr_{a}\ \mathrm{Pr}_{a} \qquad (30)$$

Stefan Boltzmann's low-temperature method was employed to compute the heat exchange coefficients for interior and exterior radiation:

$$h_{r((ext)}=\varepsilon_{g}\sigma\left[\left(T_{sky}+273\right)^{2}+\left(T_{g}+273\right)^{2}\right]\left(T_{sky}+T_{g}+546\right) \qquad (31)$$

$$h_{r(\mathrm{int})}=\varepsilon_{\mathrm{int}}\sigma\left[\left(T_{ab}+273\right)^{2}+\left(T_{g}+273\right)^{2}\right]\left(T_{ab}+T_{g}+546\right) \qquad (32)$$

$$\varepsilon_{\mathrm{int}}=\frac{\left(\frac{D_{g(\mathrm{int})}}{D_{ab(ext)}}\right)}{\left(\frac{1}{\varepsilon_{ab}}+\frac{1-\varepsilon_{g}}{\varepsilon_{g}}\right)} \qquad (33)$$

Eq. (31) was used to estimate the evolution of the ambient temperature. [46]

$$T_{a}(t)=\frac{T_{\max}+T_{\min}}{2}+\frac{T_{\max}-T_{\min}}{2}\cos\left[\frac{\pi\left(14-ST\right)}{12}\right] \qquad (34)$$

3.4. Heat Transfer: Receiver into Glass Envelope

In the defined control volume, the thermal balance between the receiver and the glass envelope is expressed as mentioned bellow[39]:

$$\left(A_{ab}\rho_{ab}Cp_{ab}\right)\frac{dT_{ab}}{dt} = A_{ab}k_{ab}\frac{d^2T_{ab}}{dx^2} + Q_{r,abs} - Q_{r-f,conv} - Q_{r-g,conv} - Q_{r-g,rad} \quad (35)$$

$$Q_{r,abs} = WI_d\rho_0\alpha_0\gamma K \quad (36)$$

The transmittance–absorptance factor is computed as stated bellow [47]:

$$\alpha_0 = \frac{\tau_g \alpha_{ab}}{1 - \left(1 - \alpha_{ab}\right)\left(1 - \tau_g\right)} \quad (37)$$

4.Computational Modelling Procedure

A fully implicit finite difference scheme is utilized to numerically resolve the governing equations, thereby guaranteeing stability amid transient operating regimes. Discretization converts the differential governing equations into a coupled system of algebraic equations, which are solved iteratively at each time step to determine the temperature distribution along the receiver and to forecast the outlet fluid temperature.

A specialized computational code was implemented in MATLAB to execute the numerical solution procedure and to conduct theoretical calculations under varying operating conditions[22]:

$$Deviation\ (\%) = \left|\left(X_{num} - X_{exp}\right) / X_{exp}\right| \times 100 \quad (38)$$

The model was considered acceptable when the deviation remained within 5–6%.

To validate the model, numerical predictions were benchmarked against empirical measurements, thereby assessing the fidelity of the proposed framework and its capacity to faithfully reproduce the thermal efficiency of the PTC.

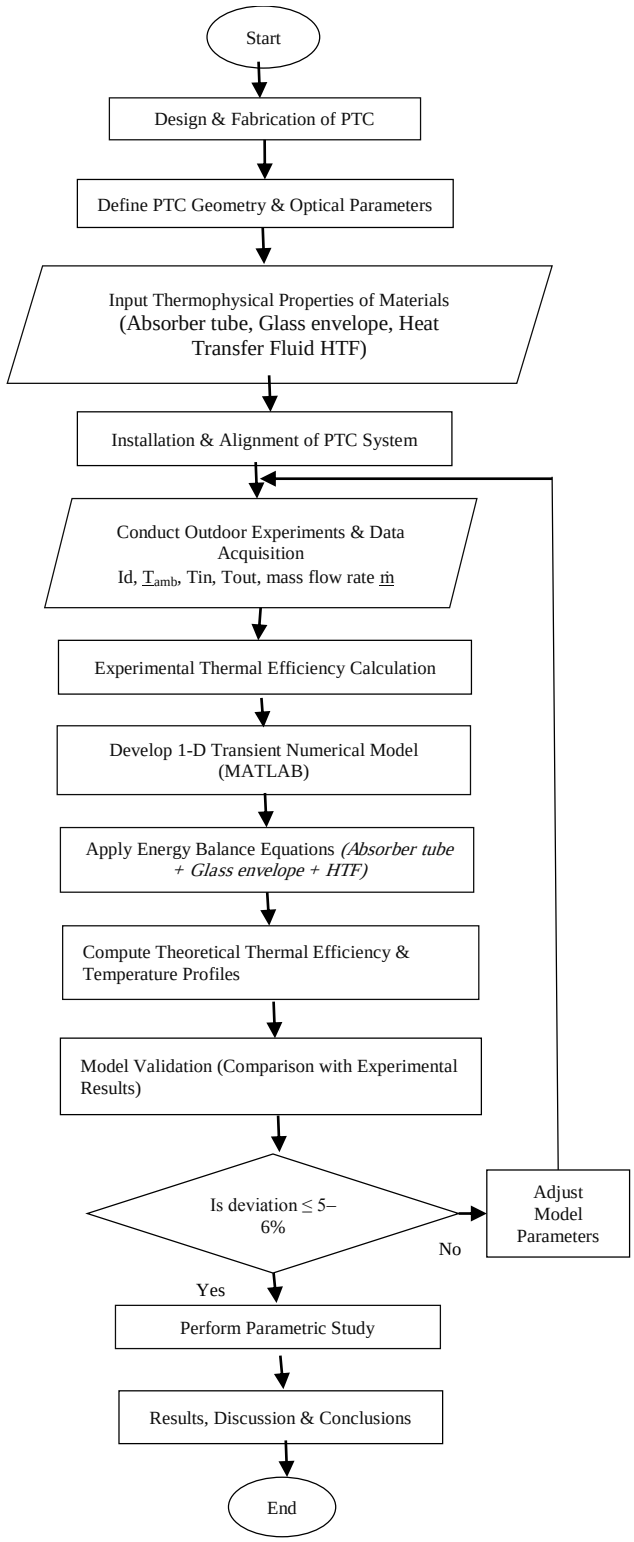

Figure 4. Flowchart Illustrating the Integrated practical and computationql Methodology of the PTC System

5. Results and Discussion

Figure ٤ exhibited the fluctuations of thermal efficiency throughout the day for both experimental and theoretical results. The efficiency increases steadily from morning hours, reaching a peak value of approximately 0.80 around solar noon (12:00–13:00 h), corresponding to maximum solar irradiation.

After midday, a gradual decline in efficiency is observed caused to the reduction in entering solar radiation and the increasing relative influence of thermal losses. The experimental and theoretical curves exhibit close agreement, with deviations remaining below 5%, indicating the reliability of the developed transient model.

The built model was validated through comparison between simulated and experimental thermal efficiency values. The deviation between both results remained below 5% throughout the day, indicating strong agreement and confirming the reliability of the model. Therefore, the model can be confidently employed to predict the thermal potency and outing water temperature under varying functioning conditions.

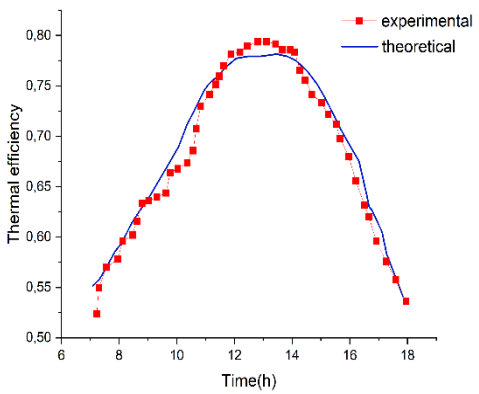

Figure 5. Water flow thermal efficiency of "0.09 kg/s

Figure 5 exhibits the fluctuation of immediate solar rays in the day on 21 June in Adrar. The irradiation increases rapidly during the morning, reaching a peak value of approximately 800 W/m² around solar noon (12:00–13:00 h), and then decreases subsequently toward the late afternoon. This behavior represents the typical diurnal solar profile and strongly affected the thermal receptivity of the PTC setup, since the heat gain is immediately dependent on the existing incident solar power. The reduction in irradiation after midday results in lower energy input and consequently decreases the collector thermal performance during afternoon hours.

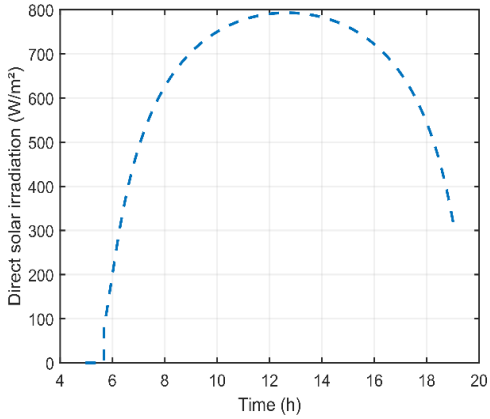

Figure 6. Water flow thermal efficiency of "0.09 kg/s

Figure ٦ presents the effect of absorber tube length on the outlet water temperature for different receiver lengths (L = 3, 5, 7, and 10 m). For all cases, the outlet temperature exhibits a progressive rise throughout the morning, attains its peak near solar noon, and subsequently declines during the afternoon in alignment with the irradiation pattern. The results indicate that increasing the absorber length significantly enhances the outlet temperature. The maximum temperature rises from approximately 45°C for L = 3 m to nearly 95°C for L = 10 m. This enhancement primarily stems from the augmented effective heat transfer surface area and the extended heat exchange pathway, facilitating increased photovoltaic energy acquisition by the receptor and improved thermal energy transduction to the active fluid.

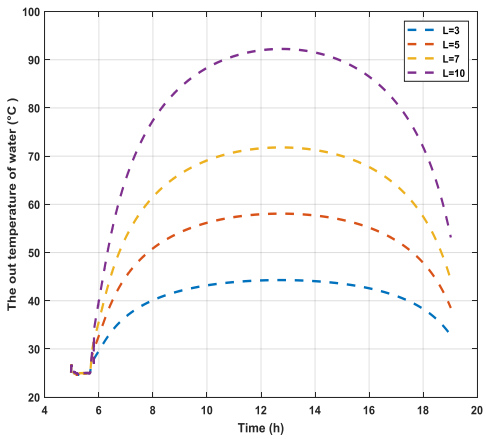

Figure 7. The heat water temperature in the 24 h for a water rate (0.1 kg/s)

Figure ٧ shows the temporal evolution of absorber temperature (Tabs), fluid temperature (Tf), and glass envelope temperature (Tg). The absorber temperature exhibits the highest values, reaching nearly 105°C around midday due to direct exposure to concentrated solar radiation. The fluid temperature remains lower, with a peak of approximately 80°C, representing the convective heat transfer occurring within the absorber tube. Meanwhile, the glass envelope temperature stays significantly lower and reaches a maximum of about 60°C, confirming its role in reducing heat losses to the environment. The temperature differential between Tabs and Tf constitutes the primary driving force for heat transfer to the fluid, while the relatively low Tg values indicate that the glass cover effectively limits thermal dissipation through convection and radiation.

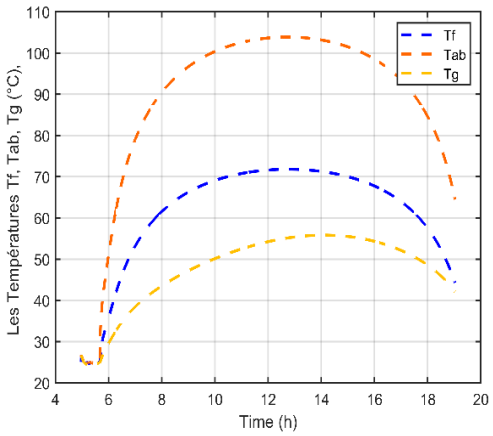

Figure 8. variation of Fluid, Absorber, and Glass Cover Temperatures in a PTC.

Figure 8 illustrates the influence of debit rate on the temperature of expulsed water in the PTC system of the debit rate examined, 0.1 kg/s produced the max outlet temperature, reaching approximately 77°C near solar noon. This outcome stems from the elongated habitancy duration of the liquid in the absorber tube, thereby promoting greater heat absorption. Although elevated mass flow rates enhance internal convective heat transfer, they concurrently limit the fluid temperature rise due to reduced heat exchange duration. Across the tested range, 0.1 kg/s offers the optimal trade-off between efficient heat absorption and thermal

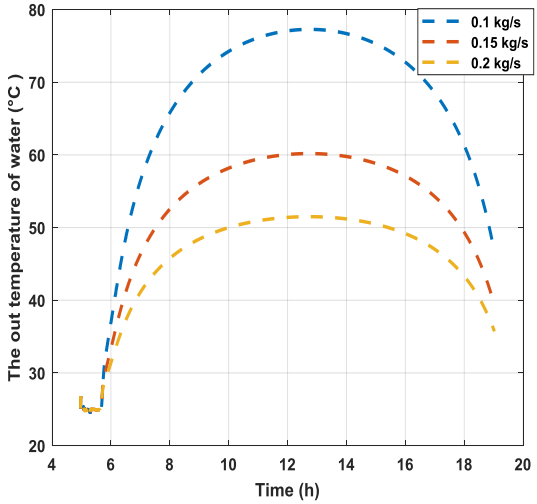

Figure 9. The heat water temperature during the day for length 6m.

Finally, Table 2 compares the present PTC system with previously published water‑heating PTC studies, such as that reported in [48] (7.8 m × 5 m), achieved relatively high efficiency (70.93%) and higher mass debit (0.345 kg/s), reflecting the capability of larger collectors to intercept greater amounts of solar radiation.

However, the study in[49] , although reporting a higher outlet water temperature (104 °C), exhibited lower thermal efficiency (53.4%). This suggests that elevated operating temperatures may intensify thermal losses, thereby reducing overall efficiency.

In contrast, the results reported in[50] demonstrated that smaller systems can achieve competitive efficiencies (66.3–68.8%) when operating within moderate temperature ranges. These findings highlight the inherent trade-off between collector size, mass flow rate, operating temperature, and thermal efficiency.

The present system achieves efficiency values comparable to those reported for larger installations, while maintaining moderate dimensions and mass flow rate. This indicates a balanced thermal performance suitable for practical applications.

Table 2. The findings of studies on heating water via Parabolic Trough Collectors (PTC)

References	Mass flow rate ($kg \cdot s^{-1}$)	Dimension of PTC	Temperature (°C)	Efficiency (%)
Ref.[50]	0.00111	1.82 m * 1.03 m	50 °C	49 %
Ref.[49]	0.00111	1.49 m2	104 °C	53.4 %
Ref.[48]	0.345	7.8 m x 5 m	47.24 °C	70.93 %
Our work	0.09	1.4m x 0.9 m	75 °C	75 - 80 %

6. Conclusions

This study presented both experimental and computed investigations of a PTC (parabolic trough collector) operating under real-time climatic conditions. A transient one-dimensional heat transfer model was developed and validated using experimental data. The comparison between theoretical predictions and experimental measurements showed good agreement, with a deviation in thermal efficiency below 5%, confirming the reliability of the proposed model.

The findings demonstrated that the receptor thermal performance is significantly influenced by the operating debit. Lower mass flow rates produced higher outlet water temperatures due to increased residence time in the inner receiver tube. Within the investigated range, a mass flow rate of 0.1 kg/s provided the most favorable compromise between heat absorption and stable thermal response.

In addition, the numerical model can be used as an effective tool to optimize the PTC design parameters and operating conditions for hot water production in residential and commercial applications. The study also confirms that water represents an appropriate heat transfer fluid because of its availability, economic advantage, and adequate thermal characteristics, making the proposed system promising for medium-temperature solar thermal applications.

Future work should focus on developing a more advanced model that incorporates thermal energy storage (TES) to improve system reliability and extend operation time. Further investigations are also recommended to evaluate alternative heat transfer fluids and absorber materials in order to enhance system productivity. Finally, implementing an automated dual-axis tracking system could significantly improve solar energy capture and overall collector performance.

Acknowledgements

This research was conducted at the Renewable Energy Research Unit in the Saharan Environment (URERMS), Adrar, Algeria. The authors appreciate the colleagues of the unit who conferred dept guidance and knowledge that assisted the research.

Nomenclature

A	Cross sectional area (m^2)
C	Specific heat (J/kg. K)
D	Diameter (m)
h	heat transfer coefficients (W/m^2)
$I0$	Solar constant
Id	Direct solar radiation(W/m^2)
K	Incident angle modifier
k	Thermal conductivity (W/m. K)
L	Absorber length (m)
m	mass(kg)
m_f	Mass flow rate(kg/s)
m_A	Atmospheric masse
Nu	Nusselt number
Pr	Prandtl number
Q	Heat flow (W)
Ra	Rayleigh number
Re	Reynolds number
T	temperature(C)
T_L	Link turbidity factor
Greek	
a	Absorptance factor
a_0	Transmittance absorptance factor
γ	Shape factor
τ	Transmittance factor
ρ_0	Reflected surface reflectivity
ρ	density(kg/m3)
δ_R	Integral Rayleigh optical thickness
θ	Incidence angle(rad)
subscripts	

a	ambient
abs	Absorber pipe
air	air
conv	convection
ext	exterior
eff	effective
f	fluid
g	Glass envelope
int	interior
lam	laminar
max	maximum
min	minimum
r	receiver
rad	radiation
s_a	Surrounding air
s	sky

References

1. Bilgen, S. (2014). Structure and environmental impact of global energy consumption. *Renewable and Sustainable Energy Reviews, 38*, 890–902. https://doi.org/10.1016/j.rser.2014.07.004.
2. Ellabban, O., Abu-Rub, H., & Blaabjerg, F. (2014). Renewable energy resources: Current status, future prospects and their enabling technology. *Renewable and Sustainable Energy Reviews, 39*, 748–764. https://doi.org/10.1016/j.rser.2014.07.113
3. Ukoba, K., Yoro, K. O., Eterigho-Ikelegbe, O., Ibegbulam, C., & Jen, T.-C. (2024). Adaptation of solar energy in the Global South: Prospects, challenges and opportunities. *Heliyon, 10*(7), e28009. https://doi.org/10.1016/j.heliyon.2024.e28009
4. Hajou, A., & El Mghouchi, Y. (2025). Solar energy potential assessment in the MENA and Mediterranean regions. *Journal of King Saud University – Engineering Sciences, 37*(7), 42. https://doi.org/10.1007/s44444-025-00052-4
5. Teggar, M., Elbar, A., Laouer, A., Atia, A., Mechraoui, A., Mekhilef, S., Ismail, K. A. R., Mezaache, E. H., Souici, M., & Lino, F. A. M. (2024). Challenges and prospects of concentrated solar power deployment in Algeria. *European Journal of Sustainable Development Research, 8*(4), em0269. https://doi.org/10.29333/ejosdr/15137.
6. Boukelia, T. E., & Mecibah, M. S. (2013). Parabolic trough solar thermal power plant: Potential and projects development in Algeria. *Renewable and Sustainable Energy Reviews*. https://doi.org/10.1016/j.rser.2012.11.074
7. Benchenina, Y., Zemmit, A., Bouzaki, M. M., Loukriz, A., Elsayed, S. K., Alzaed, A., Ali, G., & Ghoneim, S. S. M. (2025). Advancing green hydrogen production in Algeria with opportunities and challenges for future directions. *Scientific Reports, 15*(1), 5559. https://doi.org/10.1038/s41598-025-90336-1
8. Eze, F., Egbo, M., Anuta, U. J., Ntiriwaa, O.-B. R., Ogola, J., & Mwabora, J. (2024). A review on solar water heating technology: Impacts of parameters and techno-economic studies. *Bulletin of the National Research Centre, 48*, 29. https://doi.org/10.1186/s42269-024-01187-1
9. Zhang, H., Baeyens, J., Cáceres, G., Degrève, J., & Lv, Y. (2016). Thermal energy storage: Recent developments and practical aspects. *Progress in Energy and Combustion Science, 53*, 1–40. doi:10.1016/j.pecs.2015.10.003
10. Jaramillo, O. A., Venegas-Reyes, E., Aguilar, J. O., Castrejón-García, R., & Sosa-Montemayor, F. (2013). Parabolic trough concentrators for low enthalpy processes. *Renewable Energy, 60*, 529–539. doi:10.1016/j.renene.2013.04.019
11. Beemkumar, N., Yuvarajan, D., Karthikeyan, A., & Ganesan, S. (2019). Comparative experimental study on parabolic trough collector integrated with thermal energy storage system by using different reflective materials. *Journal of Thermal Analysis and Calorimetry, 137*(3), 941–948. doi:10.1007/s10973-018-07989-6
12. Kumar, G., Galphade, A., Solanki, A., BN, S., & Vasava, K. (2025). A Comparative Analysis of Standard and Flat Reflector Integrated Parabolic Trough Solar Collectors for Hot Water Generation. *Journal of Solar Energy Research, 10*(Emerging Trends in Photothermal Conversion for Solar Energy Harvesting), 1–11. https://doi.org/10.22059/jser.2025.379565.1440

13. Agagna, B., Behar, O., & Smaili, A. (2022). Performance analysis of parabolic trough solar collector under varying optical errors. *Energy Sources, Part A: Recovery, Utilization, and Environmental Effects*, *44*(1), 1189–1207. doi:10.1080/15567036.2022.2052385
14. Chakraborty, O. (2025). Improving heat transfer in parabolic trough collectors using hybrid nanofluids and concentric tube designs. *Journal of Thermal Analysis and Calorimetry*, *150*(24), 20203–20223. doi:10.1007/s10973-025-14991-2
15. Sagade, A. A., Aher, S., & Shinde, N. N. (2013). Performance evaluation of low-cost FRP parabolic trough reflector with mild steel receiver. *International Journal of Energy and Environmental Engineering*, *4*(1), 1–8. https://doi.org/10.1186/2251-6832-4-5.
16. Masrie, F., Delele, M. A., Fanta, S. W., Tesema, E. A., Alemayehu, M., Adgo, E., & Hailemariam, F. (2025). Development and performance evaluation of parabolic solar cooker for tomato paste production. *Applied Food Research*, *5*(2), 101121. https://doi.org/10.1016/j.afres.2025.101121
17. Shafiey Dehaj, M., Rezaeian, M., Mousavi, D., Shamsi, S., & Salarmofrad, M. (2021). Efficiency of the parabolic through solar collector using NiFe2O4/Water nanofluid and U-tube. *Journal of the Taiwan Institute of Chemical Engineers*, *120*, 136–149. doi:10.1016/j.jtice.2021.02.029.
18. Hosseini, S. M. S., & Shafiey Dehaj, M. (2021). Assessment of TiO2 water-based nanofluids with two distinct morphologies in a U type evacuated tube solar collector. *Applied Thermal Engineering*, *182*, 116086. doi:10.1016/j.applthermaleng.2020.116086
19. Rezaeian, M., Shafiey Dehaj, M., Zamani Mohiabadi, M., Salarmofrad, M., & Shamsi, S. (2021). Experimental investigation into a parabolic solar collector with direct flow evacuated tube. *Applied Thermal Engineering*, *189*, 116608. https://doi.org/10.1016/j.applthermaleng.2021.116608.
20. Yahi, F., Belhamel, M., Bouzeffour, F., & Sari, O. (2020). Structured dynamic modeling and simulation of parabolic trough solar collector using bond graph approach. *Solar Energy*, *196*, 27–38. https://doi.org/10.1016/j.solener.2019.11.065
21. Pal, R. K., & Kumar, K. R. (2021). Two-fluid modeling of direct steam generation in the receiver of parabolic trough solar collector with non-uniform heat flux. *Energy*, *226*, 120308. https://doi.org/10.1016/j.energy.2021.120308
22. Behar, O., Khellaf, A., & Mohammedi, K. (2015). A novel parabolic trough solar collector model – Validation with experimental data and comparison to Engineering Equation Solver (EES). *Energy Conversion and Management*, *106*, 268–281. doi:10.1016/j.enconman.2015.09.045
23. Kalogirou, S. A. (2012). A detailed thermal model of a parabolic trough collector receiver. *Energy*, *48*(1), 298–306. doi:10.1016/j.energy.2012.06.023
24. Mostafavi Tehrani, S. S., & Taylor, R. A. (2016). Off-design simulation and performance of molten salt cavity receivers in solar tower plants under realistic operational modes and control strategies. *Applied Energy*, *179*, 698–715. doi:10.1016/j.apenergy.2016.07.032
25. Otanicar, T. P., Theisen, S., Norman, T., Tyagi, H., & Taylor, R. A. (2015). Envisioning advanced solar electricity generation: Parametric studies of CPV/T systems with spectral filtering and high temperature PV. *Applied Energy*, *140*, 224–233. doi:10.1016/j.apenergy.2014.11.073
26. Fuqiang, W., Ziming, C., Jianyu, T., Yuan, Y., Yong, S., & Linhua, L. (2017). Progress in concentrated solar power technology with parabolic trough collector system: A comprehensive review. *Renewable and Sustainable Energy Reviews*, *79*, 1314–1328. doi:10.1016/j.rser.2017.05.174
27. Salgado Conrado, L., Rodriguez-Pulido, A., & Calderón, G. (2017). Thermal performance of parabolic trough solar collectors. *Renewable and Sustainable Energy Reviews*, *67*, 1345–1359. doi:10.1016/j.rser.2016.09.071
28. Colangelo, G., Favale, E., de Risi, A., & Laforgia, D. (2013). A new solution for reduced sedimentation flat panel solar thermal collector using nanofluids. *Applied Energy*, *111*, 80–93. doi:10.1016/j.apenergy.2013.04.069
29. Patil, R. G., Kale, D. M., Panse, S. V., & Joshi, J. B. (2014). Numerical study of heat loss from a non-evacuated receiver of a solar collector. *Energy Conversion and*

Management, 78, 617–626. doi:10.1016/j.enconman.2013.11.034

30. Mohamed, A. M. I., & El-Minshawy, N. A. (2011). Theoretical investigation of solar humidification–dehumidification desalination system using parabolic trough concentrators. *Energy Conversion and Management, 52*(10), 3112–3119. doi:10.1016/j.enconman.2011.04.026
31. Lobón, D. H., Valenzuela, L., & Baglietto, E. (2014). Modeling the dynamics of the multiphase fluid in the parabolic-trough solar steam generating systems. *Energy Conversion and Management, 78*, 393–404. doi:10.1016/j.enconman.2013.10.072
32. Wang, P., Liu, D. Y., & Xu, C. (2013). Numerical study of heat transfer enhancement in the receiver tube of direct steam generation with parabolic trough by inserting metal foams. *Applied Energy, 102*, 449–460. doi:10.1016/j.apenergy.2012.07.026
33. AbdelFatah, R. T., Shalaby, R., Fahim, I. S., & Kasem, M. M. (2026). Optimized control, and experimental validation of a novel multi-stage parabolic trough collector for solar water heating systems. *Sci Rep, 16*(1), 3054. doi:10.1038/s41598-025-34564-5
34. Kim, H., Chinnasamy, V., Ham, J., & Cho, H. (2025). Parabolic trough collectors: A comprehensive review of design innovations, optimization studies and applications. *Energy Conversion and Management, 327*, 119534. doi:10.1016/j.enconman.2025.119534
35. Hashemian, N., & Noorpoor, A. (2019). Assessment and multi-criteria optimization of a solar and biomass-based multi-generation system: Thermodynamic, exergoeconomic and exergoenvironmental aspects. *Energy Conversion and Management, 195*, 788–797.https://doi.org/10.1016/j.enconman.2019.05.039
36. Zhao, K., Wang, X., Gai, Z., Qin, Y., Li, Y., & Jin, H. (2024). Enhancing the efficiency of solar parabolic trough collector systems via cascaded multiple concentration ratios. *Journal of Cleaner Production, 437*, 140665. doi:https://doi.org/10.1016/j.jclepro.2024.140665
37. Duffie, J. A., & Beckman, W. A. (2013). *Solar Engineering of Thermal Processes*: John Wiley & Sons https://doi.org/10.1002/9781118671603.
38. Ahmed, D., & Natarajan, E. (2019). Thermal performance enhancement in a parabolic trough receiver tube with internal toroidal rings: A numerical investigation. *Applied Thermal Engineering, 162*, 114224. doi:10.1016/j.applthermaleng.2019.114224
39. Marif, Y., Benmoussa, H., Bouguettaia, H., Belhadj, M. M., & Zerrouki, M. (2014). Numerical simulation of solar parabolic trough collector performance in the Algeria Saharan region. *Energy Conversion and Management, 85*, 521–529. doi:10.1016/j.enconman.2014.06.002
40. Abed, N., & Afgan, I. (2020). An extensive review of various technologies for enhancing the thermal and optical performances of parabolic trough collectors. *International Journal of Energy Research, 44*(7), 5117–5164. doi:https://doi.org/10.1002/er.5271
41. Gnielinski, V. (2013). On heat transfer in tubes. *International Journal of Heat and Mass Transfer, 63*, 134–140. doi:10.1016/j.ijheatmasstransfer.2013.04.015
42. Kasten, F. (1996). The Linke turbidity factor based on improved values of the integral Rayleigh optical thickness. *Solar Energy, 56*(3), 239–244. https://doi.org/10.1016/0038-092X(95)00114-7
43. García-Valladares, O., & Velázquez, N. (2009). Numerical simulation of parabolic trough solar collector: Improvement using counter flow concentric circular heat exchangers. *International Journal of Heat and Mass Transfer, 52*(3), 597–609. doi:10.1016/j.ijheatmasstransfer.2008.08.004
44. Padilla, R. V., Demirkaya, G., Goswami, D. Y., Stefanakos, E., & Rahman, M. M. (2011). Heat transfer analysis of parabolic trough solar receiver. *Applied Energy, 88*(12), 5097–5110. doi:10.1016/j.apenergy.2011.07.012
45. Ouagued, M., Khellaf, A., & Loukarfi, L. (2013). Estimation of the temperature, heat gain and heat loss by solar parabolic trough collector under Algerian climate using different thermal oils. *Energy Conversion and Management, 75*, 191–201. doi:10.1016/j.enconman.2013.06.011

46. Belghit, A., Belahmidi, M., Bennis, A., Boutaleb, B. C., & Benet, S. (1997). Étude numérique d'un séchoir solaire fonctionnant en convection forcée. *Revue Générale de Thermique, 36*(11), 837–850. doi:10.1016/s0035-3159(97)87754-9
47. Kalogirou, S. A. (2004). Solar thermal collectors and applications. *Progress in Energy and Combustion Science, 30*(3), 231–295. https://doi.org/10.1016/j.pecs.2004.02.001
48. Sauceda, D., Velázquez, N., García-Valladares, O., & Beltrán, R. (2011). Numerical simulation and design of a parabolic trough solar collector used as a direct generator in a solar-GAX cooling cycle? *Journal of Mechanical Science and Technology, 25*(6), 1399–1408. doi:10.1007/s12206-011-0326-y
49. Rizwan, M., Raheem Junaidi, M. A., Suleman, M., & Hussain, M. A. (2014). Experimental Verification and Analysis of Solar Parabolic Collector for Water Distillation. *International Journal of Engineering Research, 3*(10), 588–593. doi:10.17950/ijer/v3s10/1008
50. Kulkarni, H. B. (2016). Design and development of prototype cylindrical parabolic solar collector for water heating application. *International Journal of Renewable Energy Development, 5*(1), 49–55. https://doi.org/10.14710/ijred.5.1.49-55.